Mineralogical Magazine, October 2009, Vol. 73(5), pp. 855–870

Cámaraite, $Ba_3NaTi_4(Fe^{2+},Mn)_8(Si_2O_7)_4O_4(OH,F)_7$. II. The crystal structure and crystal chemistry of a new group-II Ti-disilicate mineral

F. Cámara[1,2,*,†], E. Sokolova[2,3] and F. Nieto[4]

[1] CNR – Istituto di Geoscienze e Georisorse, Unità di Pavia, Via Ferrata 1, I-27100 Pavia, Italy
[2] Department of Geological Sciences, University of Manitoba, Winnipeg, Manitoba, R3T 2N2 Canada
[3] Institute of Geology of Ore Deposits, Petrography, Mineralogy and Geochemistry, Moscow, 119017, Russia
[4] Dipartimento Mineralogia y Petrologia, Universidad de Granada, Av. Fuentenueva s/n, 18002 Granada, Spain

[*Received 18 September 2009; Accepted 21 October 2009*]

ABSTRACT

Cámaraite – ideally $Ba_3NaTi_4Fe_8^{2+}(Si_2O_7)_4O_4(OH)_4F_3$ – is triclinic, space group $C\bar{1}$, a = 10.6965(7) Å, b = 13.7861(9) Å, c = 21.478(2) Å, α = 99.345(1)º, β = 92.315(2)º, γ = 89.993(2)º, V = 3122.6(4) Å^3, Z = 4, $D_{calc.}$ = 4.018 g cm^{-3}, from the Verkhnee Espe alkaline deposit, Akjailyautas Mountains, Kazakhstan, has been solved and refined to R_1 5.87% on the basis of 6682 unique reflections ($F_o > 4\sigma F$). The crystal structure of cámaraite can be described as a combination of a TS block and an intermediate (**I**) block. The TS (titanium silicate) block consists of HOH sheets (H-heteropolyhedral, O-octahedral), and is characterized by a minimal cell based on translation vectors $\mathbf{t_1}$ and $\mathbf{t_2}$, with t_1 ~5.5 and t_2 ~7 Å and $\mathbf{t_1} \wedge \mathbf{t_2}$ close to 90º. We describe the crystal structure of cámaraite using a double minimal cell, with $2t_1$ and $2t_2$ translations. In the O sheet, there are eight [6]-coordinated M^O sites occupied mainly by Fe^{2+} and Mn, with minor Fe^{3+}, Mg, Zr, Ca and Zn with $<M^O-\varphi>$ = 2.185 Å. Eight M^O sites give, ideally Fe_8^{2+} p.f.u. In the H sheet, there are four [6]-coordinated M^H sites occupied almost solely by Ti (Ti = 4 a.p.f.u.), with $<M^H-\varphi>$ = 1.963 Å, and eight [4]-coordinated Si sites occupied solely by Si, with <Si–O> = 1.621 Å. The topology of the TS block is as in Group II of the Ti-disilicates (Ti = 2 a.p.f.u. per minimal cell) in the structure hierarchy of Sokolova (2006). There are six peripheral (P) sites, four [8–12]-coordinated Ba-dominant A^P sites, giving ideally 3 Ba p.f.u., and two [10]-coordinated Na-dominant B^P sites, giving ideally 1 Na p.f.u. There are two **I** blocks: the $\mathbf{I}_1$ block is a layer of Ba atoms (two A^P sites); the $\mathbf{I}_2$ block is a layer of Ba (two A^P sites) and Na atoms (two B^P sites). Along **c**, there are two types of linkage of TS blocks: (1) TS blocks link *via* A^P cations which constitute the $\mathbf{I}_1$ block, and (2) TS blocks link *via* common vertices of M^H octahedra (as in astrophyllite-group minerals) and A^P and B^P cations which constitute the $\mathbf{I}_2$ block. Cámaraite is the only mineral of Group II with two types of linkage of TS blocks and two types of **I** blocks in its structure. The relation of cámaraite to the Group-II minerals is discussed.

Keywords: cámaraite, titanium silicate, crystal structure, TS block, group II.

Introduction

Cámaraite from the Verkhnee Espe deposit, Akjailyautas Mountains, Kazakhstan, was described as a new mineral by Sokolova *et al.* (2009*a*). Their chemical analysis by electron microprobe gave: Nb_2O_5 1.57, SiO_2 25.25, TiO_2 15.69, ZrO_2 0.33, Al_2O_3 0.13, Fe_2O_3 2.77, FeO 16.54, MnO 9.46, ZnO 0.12, MgO 0.21, CaO

* E-mail: camara@crystal.unipv.it
† Permanent address: CNR – Istituto di Geoscienze e Georisorse, Unità di Pavia, Via Ferrata 1, I-27100 Pavia, Italy
DOI: 10.1180/minmag.2009.073.5.855

0.56, BaO 21.11, Na_2O 1.41, K_2O 0.84, H_2O 1.84, F 3.11, less O≡F 1.31, total 99.63 wt.%, where the valence states of Fe were determined by Mössbauer spectroscopy [$Fe^{3+}/(Fe^{2+} + Fe^{3+})$ = 0.13(8)] and the H_2O content was derived by crystal-structure determination (the latter issue is discussed further in this paper). Sokolova *et al.* (2009*a*) gave the following empirical and simplified formulae:

$(Ba_{2.61}K_{0.34})_{\Sigma 2.95}(Na_{0.86}Ca_{0.14})_{\Sigma 1}$
$(Ti_{3.72}Nb_{0.22}Al_{0.05})_{\Sigma 3.99}(Fe^{2+}_{4.36}Fe^{3+}_{0.66}Mn_{2.53}Mg_{0.10}$
$Zr_{0.05}Zn_{0.03}Ca_{0.05})_{\Sigma 7.78}Si_{7.97}O_{35.89}H_{3.88}F_{3.11}$,

and

$Ba_3NaTi_4(Fe^{2+},Mn)_8(Si_2O_7)_4O_4(OH,F)_7$,

$Z = 4$, on the anion basis F + O + OH = 39 a.p.f.u. (atoms per formula unit), $D_{calc.}$ = 4.018 g cm^{-3}. We will describe the crystal structure of cámaraite in accord with the work of Sokolova (2006) on titanium disilicate minerals. The structures of these minerals contain the TS (Ti-silicate) block, composed of a central trioctahedral (O) sheet and two adjacent heteropolyhedral (H) sheets of different polyhedra including (Si_2O_7) groups. These minerals are divided into four groups, characterized by different topology and stereochemistry of the TS block. Each group of structures has a different linkage of H and O sheets in the TS block, and a different arrangement of Ti (= Ti + Nb) polyhedra. In a given structure, the TS block can alternate with another block, an intermediate (**I**) block, so called because it is intercalated between two TS blocks. In Groups I, II, III and IV, Ti equals 1, 2, 3 and 4 a.p.f.u. respectively. Based on the Ti content, Sokolova *et al.* (2009*a*) considered cámaraite as a Group-II mineral, i.e. Ti = 2 a.p.f.u. We will show that in cámaraite, the topology of the linkage between the H and O sheets corresponds to that of Group-II structures.

This paper presents the structure of the cámaraite as a continuation of our work on Ti-disilicate minerals with the TS block [delindeite (Sokolova and Cámara, 2007), bornemanite (Cámara and Sokolova, 2007), lomonosovite and murmanite (Cámara *et al.*, 2008), barytolamprophyllite (Sokolova and Cámara, 2008*a*), mosandrite (Sokolova and Cámara, 2008*b*), nabalamprophyllite (Sokolova and Hawthorne, 2008*a*), nacareniobsite-(Ce) (Sokolova and Hawthorne, 2008*b*), jinshajiangite (Sokolova *et al.*, 2009*b*)]. The site nomenclature is that of Sokolova (2006).

Experimental details

Transmission electron microscopy

Crystals of cámaraite can be inhomogeneous at a very localized scale due to variations in chemical composition. For better characterization of cámaraite crystals, we collected TEM data for additional crystals from the holotype specimen with a Philips CM20 transmission electron microscope working at 200 kV with an EDAX EDS system for chemical analysis in STEM mode. The instrument has a CCD camera for acquisition of images. Samples were oriented and embedded in epoxy, thinned and doubly polished. The thin slices were glued to copper rings and thinned using a Gatan Dual ion miller until transparent to electrons.

Data collection and crystal-structure refinement

A single crystal of cámaraite was mounted on a Bruker *P*4 diffractometer with a CCD 4K Smart detector and Mo-*K*α radiation. The intensities of 28111 reflections were collected to 60º2θ using 30 s per 0.2º frame, and an empirical absorption correction (*SADABS*, Sheldrick, 1998) was applied. The refined unit-cell parameters (Table 1) were obtained from 6045 reflections with $I > 10\sigma$. The crystal structure of cámaraite was solved by direct methods with the Bruker *SHELXTL Version 5.1* system of programs (Sheldrick, 1997) and refined in space group $C\bar{1}$ to R_1 = 5.87% and a GoF of 1.178. As there were hardly any observed reflections at high 2θ, refinement of the structure was based on the intensities of 6682 unique observed reflections ($F_o > 4\sigma F$) with $-13 < h < 13$, $-17 < k < 17$, $-27 < l < 27$, $2\theta \leqslant 55º$. Scattering curves for neutral atoms were taken from the International Tables for Crystallography (1992). Site occupancies for the M^H sites were refined with the scattering curve of Ti. For the four M^H sites, site occupancies converged to 1.0 (within the estimated standard deviation – esd) and they were fixed at that value. For the M^O sites, occupied mainly by Fe^{2+} and Mn, site occupancies were refined with the scattering curve of Fe; for the **I**-block sites, site occupancies were refined with the scattering curves of Ba and Na. The $A^P(2)$ site occupancy was refined with the scattering curve of Ba and converged to 1.0 (within the esd) and the site occupancy was fixed at that value. Two sites, $A^P(4A)$ and $A^P(4B)$, are separated by 0.50–1.08 Å and can only be partly occupied. The $A^P(4A)$ and $A^P(4B)$ sites constitute the $A^P(4)$ site and we

TABLE 1. Miscellaneous refinement data for cámaraite.

a (Å)	10.6965(7)
b (Å)	13.7861(9)
c (Å)	21.478(2)
α (°)	99.345(1)
β (°)	92.315(2)
γ (°)	89.993(2)
V (Å^3)	3122.6(4)
Space group	$C\bar{1}$
Z	4
Absorption coefficient (mm^{-1})	8.04
F(000)	3543.2
$D_{calc.}$ (g cm^{-3})	4.018
Crystal size (mm)	0.03 x 0.14 x 0.14
Radiation/filter	Mo-$K\alpha$/graphite
Upper 2θ-value for structure refinement (°)	55.0
R(int) (%)	2.84
Reflections collected	28111
Independent reflections	7154
$F_o > 4\sigma\|F\|$	6682
Refinement method	Full-matrix least squares on F^2, fixed weights proportional to $1/\sigma F_o^2$
Goodness of fit on F^2	1.178
Final $R_{obs.}$ (%) $[F_o > 4\sigma\|F\|]$	5.87
R indices (all data) (%)	R_1 = 6.27 wR_2 = 12.45 GoF = 1.178

refined their site occupancies with a constraint of equal displacement parameters. The crystal chemistry of the TS-block structures allowed us to identify possible monovalent anion sites in the structure of cámaraite, labelled $X_A^O(1-4)$ and $X_M^P(1-3)$. However, there was no indication that any of these anion sites is occupied solely by F. Therefore we assumed that 4 OH groups and 3 F atoms (see general formula above) are disordered over the $X_A^O(1-4)$ and $X_M^P(1-3)$ sites and included them in the refinement with a site occupancy of 8.42 e.p.f.u. $[(4 \times 8 + 3 \times 9)/7]$. At the last stages of the refinement, seven peaks with magnitudes from 3 to 6 e^- were found in the difference-Fourier map, most of these peaks occurring in the vicinity (0.63−0.91 Å) of the Ba-dominant $A^P(1-4)$ sites. Occupancies for these subsidiary peaks SP(1−7) were refined with the scattering curve of Ba (the heaviest scattering in the structure) and displacement parameters equal to those of the $A^P(1)$ site (which is fully occupied by Ba). Refined occupancies of these subsidiary sites vary from 1 to 5%, similar to site occupancies of subsidiary peaks in another Group-II mineral − jinshajiangite − where they vary from 2 to 10% (Sokolova *et al.* 2009*b*). Details of the data collection and structure refinement are given in Table 1, final atom and subsidiary-atomic parameters are given in Table 2, selected interatomic distances and angles in Table 3, refined site-scattering values and assigned populations for selected sites in Table 4, and bond-valence values in Table 5. Lists of observed and calculated structure factors have been deposited with the Principal Editor of *Mineralogical Magazine* and are available from www.minersoc.org/pages/e_journals/dep_mat_mm.html.

Site-population assignment

The refined site-scattering values at the eight M^O sites are equal within their assigned standard deviations (Table 4), and provide no information with regard to site populations. The $<M^O-\varphi>$ distances (φ = the unspecified anion, O, OH, F)

TABLE 2. Atom coordinates and displacement parameters (Å^2) for cámaraite.

Atom	x	y	z	U_{11}	U_{22}	U_{33}	U_{23}	U_{13}	U_{12}	U_{eq}
M^O(1)	0.43483(10)	0.93864(9)	0.74206(6)	0.0078(6)	0.0135(7)	0.0140(7)	0.0049(5)	−0.0030(5)	−0.0021(4)	0.0116(4)
M^O(2)	0.43694(10)	0.18505(9)	0.74447(6)	0.0082(6)	0.0102(6)	0.0132(7)	0.0019(4)	−0.0007(4)	0.0011(4)	0.0106(4)
M^O(3)	0.18444(11)	0.31156(8)	0.73935(6)	0.0080(6)	0.0099(6)	0.0110(7)	0.0018(4)	−0.0008(4)	0.0003(4)	0.0097(4)
M^O(4)	0.68883(10)	0.06102(8)	0.74836(6)	0.0083(6)	0.0095(6)	0.0105(6)	0.0017(4)	−0.0005(4)	−0.0001(4)	0.0094(4)
M^O(5)	0.43850(10)	0.43667(9)	0.74667(6)	0.0076(6)	0.0142(7)	0.0152(7)	0.0068(5)	−0.0035(5)	−0.0024(4)	0.0120(4)
M^O(6)	0.93645(11)	0.18536(9)	0.74390(6)	0.0091(6)	0.0157(7)	0.0207(7)	−0.0039(5)	−0.0060(5)	0.0034(4)	0.0161(4)
M^O(7)	0.18740(10)	0.06414(8)	0.74976(5)	0.0072(6)	0.0103(6)	0.0096(6)	0.0013(4)	−0.0002(4)	0.0005(4)	0.0091(4)
M^O(8)	0.18618(11)	0.80846(9)	0.73804(6)	0.0077(6)	0.0106(6)	0.0119(7)	0.0017(5)	−0.0006(4)	−0.0002(4)	0.0101(4)
M^H(1)	0.13405(13)	0.91975(16)	0.10904(7)	0.0046(7)	0.0152(9)	0.0068(7)	0.0032(6)	−0.0004(5)	−0.0005(6)	0.0087(3)
M^H(2)	0.36611(13)	0.11651(15)	0.88994(7)	0.0049(7)	0.0156(9)	0.0066(7)	0.0002(6)	−0.0005(5)	−0.0001(5)	0.0092(3)
M^H(3)	0.50856(12)	0.79405(13)	0.59882(6)	0.0025(6)	0.0081(8)	0.0034(6)	0.0003(5)	−0.0009(5)	−0.0002(5)	0.0048(3)
M^H(4)	0.00852(12)	0.75532(14)	0.59945(6)	0.0032(6)	0.0051(7)	0.0029(7)	0.0001(5)	−0.0009(5)	0.0001(5)	0.0038(3)
Si(1)	0.2306(2)	0.08018(16)	0.38341(10)	0.0097(10)	0.0077(10)	0.0072(10)	0.0014(8)	−0.0001(8)	−0.0001(8)	0.0082(4)
Si(2)	0.2296(2)	0.86253(15)	0.38407(10)	0.0098(10)	0.0076(10)	0.0061(10)	0.0002(8)	0.0001(8)	0.0006(7)	0.0079(4)
Si(3)	0.1252(2)	0.73230(15)	0.87103(10)	0.0110(10)	0.0074(10)	0.0057(10)	0.0008(8)	−0.0009(8)	0.0009(8)	0.0081(4)
Si(4)	0.1249(2)	0.95336(16)	0.87138(10)	0.0124(10)	0.0087(10)	0.0054(10)	0.0010(8)	0.0004(8)	0.0016(8)	0.0088(4)
Si(5)	0.1043(2)	0.23368(15)	0.87155(10)	0.0128(10)	0.0064(10)	0.0054(10)	0.0004(8)	0.0009(8)	−0.0007(8)	0.0082(4)
Si(6)	0.6051(2)	0.95443(15)	0.87165(10)	0.0119(10)	0.0079(10)	0.0047(9)	0.0026(8)	−0.0006(8)	−0.0002(8)	0.0080(4)
Si(7)	0.2495(2)	0.92056(15)	0.61625(10)	0.0102(10)	0.0069(10)	0.0064(10)	0.0009(8)	−0.0008(8)	0.0005(8)	0.0079(4)
Si(8)	0.24927(19)	0.13881(15)	0.61685(10)	0.0079(9)	0.0071(10)	0.0073(10)	0.0017(8)	0.0005(8)	0.0012(7)	0.0074(4)
A^P(1)	0.87372(5)	0.36887(4)	0.98145(2)	0.0088(3)	0.0290(3)	0.0106(3)	0.0020(2)	0.00029(18)	−0.00086(19)	0.01629(19)
A^P(2)	0.12668(4)	0.12888(4)	0.01671(2)	0.0090(2)	0.0140(3)	0.0089(2)	0.00113(17)	−0.00020(17)	0.00063(16)	0.01072(15)
A^P(3)	½	0	½	0.0088(4)	0.004(3)	0.0039(5)	0.0011(5)	−0.0008(3)	−0.0003(5)	0.0054(13)
A^P(4A)	0.0005(4)	0.0389(9)	0.4996(4)	0.0218(12)	0.038(6)	0.0153(19)	0.005(2)	−0.0038(12)	−0.0024(17)	0.0252(19)
A^P(4B)	−0.0067(11)	−0.0046(18)	0.4886(8)	0.0218(12)	0.038(6)	0.0153(19)	0.005(2)	−0.0038(12)	−0.0024(17)	0.0252(19)
B^P(1)	¼	¼	½	0.025(2)	0.022(2)	0.004(3)	0.0007(18)	0.0010(17)	−0.0067(17)	0.0172(15)
B^P(2)	¼		½	0.026(3)	0.017(2)	0.006(2)	0.0001(16)	−0.0013(17)	0.0098(18)	0.0165(15)
O(1)	0.2684(5)	0.4287(4)	0.6933(3)	0.013(3)	0.009(3)	0.007(3)	−0.000(2)	−0.000(2)	0.000(2)	0.0098(11)
O(2)	0.1274(6)	0.1562(5)	0.4143(3)	0.013(3)	0.025(3)	0.011(3)	0.004(2)	−0.000(2)	0.002(2)	0.0163(12)
O(3)	0.1326(6)	0.3953(5)	0.5851(3)	0.011(3)	0.027(3)	0.014(3)	0.002(3)	−0.004(2)	−0.005(2)	0.0174(13)
O(4)	0.1827(6)	0.9762(4)	0.4038(3)	0.017(3)	0.013(3)	0.017(3)	0.001(2)	0.001(2)	0.002(2)	0.0156(12)
O(5)	0.2705(5)	0.6668(4)	0.6924(3)	0.008(2)	0.011(3)	0.007(3)	0.003(2)	0.000(2)	−0.001(2)	0.0082(10)
O(6)	0.3671(5)	0.8528(5)	0.4148(3)	0.008(3)	0.027(3)	0.011(3)	0.001(2)	−0.004(2)	0.006(2)	0.0157(12)
O(7)	0.1267(6)	0.8021(5)	0.4157(3)	0.012(3)	0.028(3)	0.013(3)	0.003(3)	−0.001(2)	−0.002(2)	0.0177(13)
O(8)	0.0070(6)	0.2758(5)	0.0986(3)	0.013(3)	0.024(3)	0.018(3)	−0.003(3)	0.004(2)	−0.004(2)	0.0192(13)
O(9)	0.2659(6)	0.8198(5)	1.0919(3)	0.012(3)	0.032(4)	0.014(3)	0.003(3)	0.001(2)	0.004(3)	0.0194(13)
O(10)	0.1159(5)	0.6980(4)	0.7953(3)	0.010(3)	0.011(3)	0.008(3)	−0.001(2)	0.002(2)	0.001(2)	0.0097(11)

O(11)	0.6770(6)	0.3464(4)	0.8842(3)	0.019(3)	0.013(3)	0.019(3)	0.002(2)	−0.006(3)	−0.003(2)	0.0173(13)
O(12)	0.2350(6)	0.0255(5)	0.9066(3)	0.014(3)	0.027(3)	0.017(3)	0.004(3)	0.000(2)	−0.003(3)	0.0192(13)
O(13)	0.1136(5)	0.9481(4)	0.7954(3)	0.014(3)	0.017(3)	0.005(3)	0.003(2)	0.001(2)	0.001(2)	0.0119(11)
O(14)	0.0064(5)	0.0201(5)	0.0981(3)	0.007(3)	0.032(4)	0.016(3)	0.007(3)	0.006(2)	0.008(2)	0.0176(13)
O(15)	0.1025(5)	0.2010(4)	0.7950(3)	0.013(3)	0.014(3)	0.005(3)	−0.000(2)	−0.002(2)	−0.002(2)	0.0108(11)
O(16)	0.2415(5)	0.2225(5)	0.9005(3)	0.008(3)	0.031(4)	0.017(3)	−0.005(3)	−0.005(2)	0.004(2)	0.0200(14)
O(17)	−0.0004(6)	0.1800(5)	0.9064(3)	0.011(3)	0.029(4)	0.014(3)	−0.001(3)	0.001(2)	−0.005(2)	0.0187(13)
O(18)	0.0553(6)	0.3478(4)	0.8856(3)	0.020(3)	0.014(3)	0.016(3)	0.003(2)	0.002(2)	0.000(2)	0.0164(12)
O(19)	0.2595(6)	0.0199(5)	1.0965(3)	0.013(3)	0.032(4)	0.017(3)	0.011(3)	−0.005(2)	−0.008(3)	0.0200(14)
O(20)	0.5013(6)	0.0276(5)	0.9076(3)	0.011(3)	0.026(3)	0.018(3)	0.002(3)	−0.002(2)	0.003(2)	0.0189(13)
O(21)	0.6052(5)	0.9498(4)	0.7955(3)	0.011(3)	0.012(3)	0.008(3)	0.006(2)	−0.002(2)	0.002(2)	0.0101(11)
O(22)	0.3812(5)	0.8948(5)	0.5850(3)	0.010(3)	0.028(3)	0.015(3)	0.006(3)	0.001(2)	0.006(2)	0.0174(13)
O(23)	0.2611(5)	0.9298(4)	0.6928(3)	0.009(3)	0.012(3)	0.009(3)	0.000(2)	0.001(2)	0.001(2)	0.0099(11)
O(24)	0.1414(6)	0.8439(5)	0.5844(3)	0.013(3)	0.022(3)	0.013(3)	−0.001(2)	0.003(2)	0.000(2)	0.0161(12)
O(25)	0.1985(6)	0.0251(5)	0.5971(3)	0.018(3)	0.016(3)	0.016(3)	0.001(2)	0.001(2)	0.001(2)	0.0167(12)
O(26)	0.2590(5)	0.1696(4)	0.6934(3)	0.014(3)	0.011(3)	0.005(3)	0.001(2)	0.001(2)	−0.002(2)	0.0100(11)
O(27)	0.3821(5)	0.1473(5)	0.5865(3)	0.009(3)	0.024(3)	0.013(3)	−0.001(2)	0.003(2)	−0.004(2)	0.0160(12)
O(28)	0.1418(6)	0.1984(5)	0.5841(3)	0.014(3)	0.021(3)	0.015(3)	0.003(5)	0.001(2)	0.005(2)	0.0166(13)
O(29)	0.9803(5)	0.2138(4)	0.3156(3)	0.009(3)	0.017(3)	0.007(3)	−0.003(2)	−0.002(2)	−0.002(2)	0.0116(11)
O(30)	0.1434(5)	0.9299(4)	0.1931(3)	0.009(3)	0.021(3)	0.009(3)	0.007(2)	−0.002(2)	−0.002(2)	0.0123(11)
O(31)	0.9820(5)	0.6939(5)	0.3168(3)	0.010(3)	0.026(3)	0.011(3)	0.008(3)	−0.001(2)	0.003(2)	0.0150(12)
O(32)	0.3567(5)	0.0831(4)	0.8051(3)	0.009(3)	0.021(3)	0.007(3)	−0.000(2)	0.000(2)	0.002(2)	0.0125(11)
$X^{O}_{O}(1)$	0.5121(5)	0.0515(4)	0.7001(3)	0.016(3)	0.018(3)	0.008(3)	0.000(2)	0.000(2)	−0.001(2)	0.0143(11)
$X^{O}_{O}(2)$	0.0120(5)	0.0493(4)	0.7020(3)	0.012(3)	0.017(3)	0.009(3)	0.004(2)	−0.000(2)	0.001(2)	0.0126(11)
$X^{O}_{O}(3)$	0.3609(5)	0.8231(4)	0.7847(3)							0.0118(12)
$X^{O}_{A}(4)$	0.3603(5)	0.3200(5)	0.7866(3)	0.014(3)	0.026(3)	0.016(3)	0.003(3)	0.002(2)	0.004(2)	0.0187(13)
$X^{P}_{M}(1)$	0.1272(5)	0.8999(4)	0.0105(3)							0.0145(12)
$X^{M}_{P}(2)$	0.3751(5)	0.1522(5)	0.9888(3)	0.012(3)	0.023(3)	0.003(3)	−0.003(2)	−0.001(2)	0.001(2)	0.0135(11)
$X^{M}_{P}(3)$	0.0010(5)	0.2744(5)	0.4996(2)	0.014(3)	0.010(3)	0.005(3)	0.002(2)	−0.003(2)	0.001(2)	0.0095(10)
Subsidiary peaks										
SP(1)	0.004(3)	0.222(4)	0.5010(18)	0.0088(3)	0.0290(3)	0.0106(3)	0.0020(2)	0.00029(18)	−0.00086(19)	0.01629(19)
SP(2)	0.378(3)	0.089(3)	0.9882(16)	0.0088(3)	0.0290(3)	0.0106(3)	0.0020(2)	0.00029(18)	−0.00086(19)	0.01629(19)
SP(3)	0.4998(15)	0.033(6)	0.4993(8)	0.0088(3)	0.0290(3)	0.0106(3)	0.0020(2)	0.00029(18)	−0.00086(19)	0.01629(19)
SP(4)	0.1354(17)	0.873(2)	0.1092(9)	0.0088(3)	0.0290(3)	0.0106(3)	0.0020(2)	0.00029(18)	−0.00086(19)	0.01629(19)
SP(5)	0.3660(15)	0.0650(18)	0.8888(8)	0.0088(3)	0.0290(3)	0.0106(3)	0.0020(2)	0.00029(18)	−0.00086(19)	0.01629(19)
SP(6)	0.5073(15)	0.7441(19)	0.5978(8)	0.0088(3)	0.0290(3)	0.0106(3)	0.0020(2)	0.00029(18)	−0.00086(19)	0.01629(19)
SP(7)	0.0076(13)	0.8011(17)	0.6016(7)	0.0088(3)	0.0290(3)	0.0106(3)	0.0020(2)	0.00029(18)	−0.00086(19)	0.01629(19)

TABLE 3. Selected interatomic distances (Å) and angles (º) in cámaraite.

$M^{O}(1)-O(23)$	2.094(6)	$M^{O}(2)-X_{A}^{O}(1)$	2.107(6)	$M^{O}(3)-X_{A}^{O}(4)$	2.095(6)
$M^{O}(1)-X_{A}^{O}(1)a$	2.105(6)	$M^{O}(2)-X_{A}^{O}(4)$	2.113(6)	$M^{O}(3)-O(31)e$	2.103(6)
$M^{O}(1)-O(21)$	2.106(6)	$M^{O}(2)-O(26)$	2.150(6)	$M^{O}(3)-O(26)$	2.208(6)
$M^{O}(1)-X_{A}^{O}(3)$	2.130(6)	$M^{O}(2)-O(10)c$	2.158(6)	$M^{O}(3)-O(1)$	2.231(6)
$M^{O}(1)-O(31)b$	2.251(6)	$M^{O}(2)-O(29)d$	2.253(6)	$M^{O}(3)-O(21)f$	2.267(6)
$M^{O}(1)-O(32)a$	2.391(6)	$M^{O}(2)-O(32)$	2.256(6)	$M^{O}(3)-O(15)$	2.280(6)
$\langle M^{O}(1)-\varphi\rangle$	2.180	$\langle M^{O}(2)-\varphi\rangle$	2.173	$M^{O}(3)-\varphi\rangle$	2.197
$M^{O}(4)-X_{A}^{O}(1)$	2.113(6)	$M^{O}(5)-O(13)c$	2.101(6)	$M^{O}(6)-O(15)v$	2.042(6)
$M^{O}(4)-O(30)e$	2.140(6)	$M^{O}(5)-O(1)$	2.104(6)	$M^{O}(6)-O(5)c$	2.047(6)
$M^{O}(4)-O(10)c$	2.154(6)	$M^{O}(5)-X_{A}^{O}(2)h$	2.121(6)	$M^{O}(6)-X_{A}^{O}(2)v$	2.119(6)
$M^{O}(4)-O(21)g$	2.180(5)	$M^{O}(5)-X_{A}^{O}(4)$	2.128(6)	$M^{O}(6)-X_{A}^{O}(3)c$	2.131(6)
$M^{O}(4)-O(1)c$	2.198(6)	$M^{O}(5)-O(30)i$	2.267(6)	$M^{O}(6)-O(30)e$	2.424(6)
$M^{O}(4)-O(5)c$	2.233(5)	$M^{O}(5)-O(29)d$	2.458(6)	$M^{O}(6)-O(31)j$	2.455(6)
$\langle M^{O}(4)-\varphi\rangle$	2.170	$\langle M^{O}(5)-\varphi\rangle$	2.196	$\langle M^{O}(6)-\varphi\rangle$	2.203
$M^{O}(7)-X_{A}^{O}(2)$	2.096(6)	$M^{O}(8)-O(29)e$	2.077(6)		
$M^{O}(7)-O(32)$	2.118(6)	$M^{O}(8)-X_{A}^{O}(3)$	2.079(6)		
$M^{O}(7)-O(13)g$	2.171(6)	$M^{O}(8)-O(23)$	2.231(6)		
$M^{O}(7)-O(15)$	2.191(6)	$M^{O}(8)-O(5)$	2.244(6)		
$M^{O}(7)-O(2)b$	2.194(5)	$M^{O}(8)-O(10)$	2.254(6)		
$M^{O}(7)-O(23)g$	2.212(5)	$M^{O}(8)-O(13)$	2.266(6)		
$\langle M^{O}(7)-\varphi\rangle$	2.164	$\langle M^{O}(8)-\varphi\rangle$	2.192		
$M^{H}(1)-O(30)$	1.788(6)	$M^{H}(2)-O(32)$	1.804(6)	$M^{H}(3)-O(31)b$	1.792(6)
$M^{H}(1)-O(17)k$	1.964(6)	$M^{H}(2)-O(20)$	1.961(6)	$M^{H}(3)-O(28)h$	1.941(6)
$M^{H}(1)-O(9)l$	1.975(7)	$M^{H}(2)-O(12)$	1.963(7)	$M^{H}(3)-O(7)i$	1.944(6)
$M^{H}(1)-O(14)a$	1.978(6)	$M^{H}(2)-O(16)$	1.970(7)	$M^{H}(3)-O(3)h$	1.990(6)
$M^{H}(1)-O(19)m$	1.982(6)	$M^{H}(2)-O(8)n$	1.991(6)	$M^{H}(3)-O(22)$	1.993(6)
$M^{H}(1)-X_{M}^{P}(1)$	2.088(5)	$M^{H}(2)-X_{M}^{P}(2)$	2.098(6)	$M^{H}(3)-X_{M}^{P}(3)h$	2.103(5)
$\langle M^{H}(1)-\varphi\rangle$	1.963	$\langle M^{H}(2)-\varphi\rangle$	1.965	$\langle M^{H}(3)-\varphi\rangle$	1.961
$M^{H}(4)-O(29)e$	1.803(6)	$Si(1)-O(3)n$	1.599(6)	$Si(2)-O(6)$	1.602(6)
$M^{H}(4)-O(2)k$	1.941(6)	$Si(1)-O(2)$	1.610(6)	$Si(2)-O(7)$	1.616(6)
$M^{H}(4)-O(24)$	1.944(6)	$Si(1)-O(1)n$	1.633(6)	$Si(2)-O(5)i$	1.627(6)
$M^{H}(4)-O(27)p$	1.991(6)	$Si(1)-O(4)g$	1.653(6)	$Si(2)-O(4)$	1.639(6)
$M^{H}(4)-O(6)i$	1.992(6)	$\langle Si(1)-O\rangle$	1.624	$\langle Si(2)-O\rangle$	1.621
$M^{H}(4)-X_{M}^{P}(4)k$	2.098(5)				
$\langle M^{H}(4)-\varphi\rangle$	1.962				
$Si(3)-O(8)k$	1.592(6)	$Si(4)-O(14)k$	1.592(6)	$Si(5)-O(16)$	1.588(6)
$Si(3)-O(9)r$	1.617(7)	$Si(4)-O(13)$	1.622(6)	$Si(5)-O(17)$	1.616(6)
$Si(3)-O(10)$	1.617(6)	$Si(4)-O(12)a$	1.623(7)	$Si(5)-O(15)$	1.633(6)
$Si(3)-O(11)p$	1.644(6)	$Si(4)-O(11)p$	1.637(6)	$Si(5)-O(18)$	1.642(6)
$\langle Si(3)-O\rangle$	1.618	$\langle Si(4)-O\rangle$	1.619	$\langle Si(5)-O\rangle$	1.620
$Si(6)-O(19)s$	1.592(6)	$Si(7)-O(22)$	1.600(6)	$Si(8)-O(27)$	1.598(6)
$Si(6)-O(21)$	1.627(6)	$Si(7)-O(24)$	1.620(6)	$Si(8)-O(28)$	1.617(6)
$Si(6)-O(20)a$	1.631(7)	$Si(7)-O(23)$	1.628(6)	$Si(8)-O(26)$	1.630(6)
$Si(6)-O(18)h$	1.641(6)	$Si(7)-O(25)a$	1.648(6)	$Si(8)-O(25)$	1.643(7)
$\langle Si(6)-O\rangle$	1.623	$\langle Si(7)-O\rangle$	1.624	$\langle Si(8)-O\rangle$	1.622

$Si(1)a-O(4)-Si(2)$	131.6(4)
$Si(3)c-O(11)-Si(4)c$	136.4(4)
$Si(5)-O(18)-Si(6)f$	135.9(4)
$Si(7)g-O(25)-Si(8)$	132.0(4)
$\langle Si-O-Si\rangle$	134.0

Table 3 (*contd.*)

$A^P(1)-X^P_M(1)t$	2.752(6)	$A^P(2)-X^P_M(1)x$	2.769(6)	$A^P(3)-O(6)e$	2.841(6) ×2
$A^P(1)-X^P_M(2)u$	2.763(6)	$A^P(2)-X^P_M(2)l$	2.778(6)	$A^P(3)-O(3)c$	2.843(6) ×2
$A^P(1)-O(20)u$	2.854(7)	$A^P(2)-O(19)l$	2.803(6)	$A^P(3)-O(22)g$	2.846(6) ×2
$A^P(1)-O(9)c$	2.857(6)	$A^P(2)-O(8)$	2.804(6)	$A^P(3)-O(27)$	2.851(6) ×2
$A^P(1)-O(18)v$	2.868(6)	$A^P(2)-O(16)n$	2.822(6)	$A^P(3)-X^P_{M(3)c}$	3.108(6) ×2
$A^P(1)-O(11)$	2.884(6)	$A^P(2)-O(14)$	2.828(6)	$<A^P(3)-\varphi>$	2.898
$A^P(1)-O(9)s$	3.155(7)	$A^P(2)-O(12)l$	2.845(7)		
$A^P(1)-O(17)v$	3.163(7)	$A^P(2)-O(17)l$	2.871(6)		
$A^P(1)-O(12)h$	3.222(7)	$A^P(2)-X^PM(2)n$	3.040(7)		
$A^P(1)-O(20)h$	3.236(7)	$A^P(2)-X^P_M(1)$	3.138(7)		
$A^P(1)-O(19)h$	3.242(7)	$A^P(2)-O(14)y$	3.225(7)		
$A^P(1)-O(8)w$	3.283(7)	$A^P(2)-O(16)l$	3.270(7)		
$<A^P(1)-\varphi>$	3.023	$<A^P(2)-\varphi>$	2.932		
$A^P(4A)-O(4)g$	2.919(8)	$A^P(4B)-O(25)z$	2.68(2)	$A^P(4A)-A^P(4A)z$	1.08(2)
$A^P(4A)-O(4)k$	2.943(8)	$A^P(4B)-O(4)g$	2.76(1)	$A^P(4A)-A^P(4B)z$	0.57(2)
$A^P(4A)-O(25)z$	2.945(9)	$A^P(4B)-O(4)k$	3.02(1)	$A^P(4A)-A^P(4B)$	0.61(2)
$A^P(4A)-O(25)$	2.947(9)	$A^P(4B)-O(25)$	3.11(2)	$A^P(4B)-A^P(4B)z$	0.50(3)
$A^P(4A)-O(7)k$	2.98(1)	$A^P(4B)-O(28)z$	3.18(2)		
$A^P(4A)-O(24)k$	2.98(1)	$A^P(4B)-O(7)g$	3.23(2)		
$A^P(4A)-O(28)$	2.98(1)	$A^P(4B)-O(24)k$	3.22(2)		
$A^P(4A)-O(2)$	3.00(1)	$A^P(4B)-O(2)$	3.30(2)		
$A^P(4A)-X^P_M(3)$	3.25(1)	$<A^P(4B)-O>$	3.06		
$<A^P(4A)-O>$	2.99				
$B^P(1)-O(28)$	2.387(6) ×2	$B^P(2)-O(24)$	2.393(6) ×2		
$B^P(1)-O(2)$	2.411(6) ×2	$B^P(2)-O(7)$	2.401(6) ×2		
$B^P(1)-X^P_M(3)$	2.685(5) ×2	$B^P(2)-X^P_M(3)$	2.706(5) ×2		
$B^P(1)-O(3)$	2.816(6) ×2	$B^P(2)-O(22)$	2.810(7) ×2		
$B^P(1)-O(27)$	2.845(6) ×2	$B^P(2)-O(6)$	2.820(6) ×2		
$<B^P(1)-\varphi>$	2.629	$<B^P(2)-\varphi>$	2.626		

a: *x*, *y*+1, *z*; b: −*x*+3/2, −*y*+3/2, −*z*+1; c: *x*+1/2, *y*−1/2, *z*; d: −*x*+3/2, −*y*+1/2, −*z*+1; e: −*x*+1, −*y*+1, −*z*+1; f: *x*−1/2, *y*−1/2, *z*; g: *x*, *y*−1, *z*; h: *x*+1/2, *y*+1/2, *z*; i: −*x*+1/2, −*y*+3/2, −*z*+1; j: −*x*+2, −*y*+1, −*z*+1; k: −*x*, −*y*+1, −*z*+1; l: *x*, *y*, *z*−1; m: *x*, *y*+1, *z*−1; n: −*x*+1/2, −*y*+1/2, −*z*+1; o: −*x*, −*y*+1, −*z*+1; p: *x*−1/2, *y*+1/2, *z*; r: −*x*+1/2, −*y*+3/2, −*z*+2; s: −*x*+1, −*y*+1, −*z*+2; t: *x*+1/2, *y*−1/2, *z*+1; u: −*x*+3/2, −*y*+1/2, −*z*+2; v: *x*+1, *y*, *z*; w: *x*+1, *y*, *z*+1; x: −*x*, −*y*+1, −*z*; y: −*x*, −*y*, −*z*; z: −*x*, −*y*, −*z*+1

vary from 2.164 to 2.203 Å in accord with the dominance of Fe^{2+} (4.36 a.p.f.u.; r = 0.78 Å, Shannon 1976) and Mn (2.53 a.p.f.u.; r = 0.83 Å); this variation suggests some order of Fe^{2+} and Mn into the smaller and larger polyhedra respectively, but does not provide sufficient information for the assignment of quantitative site-populations. Therefore, we consider eight Fe^{2+}-dominant M^O sites with a bulk composition 4.36 Fe^{2+} + 2.53 Mn + 0.66 Fe^{3+} + 0.10 Mg + 0.05 Zr + 0.05 Ca + 0.03 Zn + 0.22 □ p.f.u.

In cámaraite, there are six peripheral sites, $A^P(1-4)$ and $B^P(1,2)$. The numbers of $A^P(1)$, $A^P(2)$, $A^P(3)$ and $A^P(4)$ sites in the formula unit are 1, 1, 0.50 and 1 respectively (Table 3). The $A^P(4)$ site splits into two sites, $A^P(4A)$ and $A^P(4B)$, with separations $A^P(4A)-A^P(4A)' = 1.08$ Å, $A^P(4B)-A^P(4B)' = 0.50$ Å (Table 3) and $A^P(4A)-A^P(4B) = 0.57$ and 0.61 Å (Table 3). Therefore, four positions at the $A^P(4)$ site form a quadruplet where any position is surrounded by three positions at short distances of 0.5 to 1.08 Å (Table 3). Hence, the $A^P(4A)$ and $A^P(4B)$ sites can be only 25% occupied and the $A^P(4)$ site can be only 50% occupied. The resulting number of A^P cations is 1 + 1 + 0.50 + 0.5 = 3.0 a.p.f.u. The cations to be assigned to the A^P and B^P are Ba, K, Na and Ca [table 1 in (Sokolova *et al.* 2009*a*)]. The $<A^P-O>$ and $<B^P-O>$ distances are within the ranges 2.898−3.06 and 2.626−2.629 Å respectively. On the basis of their relative cation radii (Shannon, 1976), Ba and K were assigned to

TABLE 4. Refined site-scattering (e.p.f.u.) and assigned site-populations (a.p.f.u.) for cámaraite.

Site	Refined site-scattering	Site population	Calculated site-scattering	$\langle X-\varphi\rangle_{calc.}$* (Å)	$\langle X-\varphi\rangle_{obs.}$ (Å)
$M^O(1)$	25.7(2)	4.36 Fe^{2+} + 2.53 Mn + 0.66 Fe^{3+} + 0.10 Mg + 0.05 Zr + 0.05 Ca + 0.03 Zn + 0.22 □			2.180
$M^O(2)$	25.6(2)				2.173
$M^O(3)$	25.4(2)				2.198
$M^O(4)$	25.8(2)				2.170
$M^O(5)$	25.6(2)				2.196
$M^O(6)$	26.0(2)				2.203
$M^O(7)$	25.7(2)				2.164
$M^O(8)$	25.5(2)				2.192
ΣM^O	205.3		198.87	2.150	2.185**
$M^H(1)$	22.0	3.72 Ti + 0.22 Nb + 0.05 Al			1.963
$M^H(2)$	22.0				1.965
$M^H(3)$	22.0				1.961
$M^H(4)$	22.0				1.962
ΣM^H	88.0		91.51	1.975	1.963**
$^{[12]}A^P(1)$	55.4(2)	1.0 Ba	56.0	2.978	3.023
$^{[12]}A^P(2)$	56.0	1.0 Ba	56.0	2.973	2.932
$^{[10]}A^P(3)$	23(1)	0.36 Ba + 0.14 K	22.8	2.913	2.898
$^{[9]}A^P(4A)$	12.8(4)	0.25 Ba + 0.75 □	14.0	2.85	2.99
$^{[8]}A^P(4B)$	5.5(4)	0.20 K + 0.80 □	3.8	2.89	3.06
ΣA^P	152.7	2.61 Ba + 0.34 K	152.6		2.97**
$^{[10]}B^P(1)$	6.2(1)	0.43 Na + 0.07 Ca	6.1	2.654	2.629
$^{[10]}B^P(2)$	6.1(1)	0.43 Na + 0.07 Ca	6.1	2.654	2.626
ΣB^P	12.3	0.86 Na + 0.14 Ca	12.2		2.628**

* X-cation, φ-anion: ionic radii are from Shannon (1976); $\langle X-\varphi\rangle_{calc} = r_{cat} + \langle r_{anion}\rangle$ where $\langle r_{anion}\rangle$ for an individual polyhedron has been calculated taking into account that:
(1) all O atoms are [4]-coordinated except for [3]-coordinated O(11) and O(18);
(2) $X^O_A(1-4)$ and $X^P_M(1-3)$ atoms are each occupied by $[(OH)_{4/7}F_{3/7}]$;
(3) $X^O_A(1-4)$, $X^P_M(1,2)$ and $X^P_M(3)$ atoms are [3]-, [4]- and [6]-coordinated respectively.
** mean $\langle X-\varphi\rangle_{obs}$ for a group of cations.

the A^P sites, and Na and minor Ca were assigned to the B^P sites, and the resulting aggregate site-populations are in accord with the aggregate refined site-scattering values (Table 4). At the A^P sites, the maximum refined site-scattering values are at the $A^P(1)$ and $A^P(2)$ sites: 55.4 and 56 e.p.f.u. (Table 4) for a site multiplicity of 1; thus we assign these sites as filled completely with Ba. This leaves three species, Ba, K and □, to be assigned to the $A^P(3)$ and $A^P(4)$ sites. The refined site-scattering values indicate that Ba is dominant at $A^P(3)$. The site scattering at the $A^P(4A)$ and $A^P(4B)$ sites are 12.8(4) and 5.5(4) e.p.f.u., the $A^P(4A)$ and $A^P(4B)$ sites can be only 25% occupied (see discussion above), and therefore we assign 0.75 □ + 0.25 Ba to the $A^P(4A)$ site and 0.80 □ + 0.20 K to the $A^P(4B)$ site (Table 4).

The refined site-scattering values at the B^P sites indicate identical occupancies, and Na and Ca were assigned on this basis (Table 5).

Description of the structure

Cation sites

We divide the cation sites into three groups: M^O sites of the O sheet, M^H and Si sites of the H sheet, and peripheral A^P and B^P sites which constitute the **I** block. Also in accord with Sokolova (2006), we label specific anions X^O and X^P (anions of the O sheet and peripheral anions); X^O_M = common vertices of M^O and M^H polyhedra; X^O_A = common vertices of M^O and A^P polyhedra; X^P_M = apical anions of M^H polyhedra at the periphery of the TS block. We will describe

the composition of each structural fragment within a planar cell that is double (on each axis) the planar cell common to Ti-disilicate minerals with the TS block: a planar cell is based on translation vectors $\mathbf{t_1}$ and $\mathbf{t_2}$ with t_1 ~5.5 and t_2 ~7 Å and $\mathbf{t_1} \wedge \mathbf{t_2}$ close to 90º (Sokolova, 2006); the double planar cell for cámaraite is based on translation vectors, $2\mathbf{t_1}$ and $2\mathbf{t_2}$, and was chosen in order to facilitate comparison with other Group II minerals.

O sheet

There are eight [6]-coordinated M^O sites in the O sheet (Tables 2, 3, 4). The $M^O(1-8)$ sites are occupied mainly by Fe^{2+} and Mn, with minor Fe^{3+}, Mg, Zr, Ca and Zr (table 1 in Sokolova *et al*., 2009*a* and Table 4). The $M^O(1,2,5,6)$ atoms are coordinated by four O atoms and two monovalent anions, X^O_A (see discussion below), with $<M^O(1,2,5,6)-\varphi> = 2.180$, 2.173, 2.196 and 2.203 Å respectively. The $M^O(3,4,7,8)$ atoms are coordinated by five O atoms and a monovalent X^O_A anion, with $<M^O(3,4,7,8)-\varphi> = 2.197$, 2.170, 2.164 and 2.192 Å. The eight [6]-coordinated M^O sites contain 4.36 Fe^{2+} + 2.53 Mn + 0.66 Fe^{3+} + 0.10 Mg + 0.05 Zr + 0.05 Ca + 0.03 Zn + 0.22 □ p.f.u = 8 a.p.f.u., ideally Fe^{2+}_8 p.f.u.

H sheet

There are four [6]-coordinated M^H sites in the H sheet, and these are occupied almost solely by Ti (Tables 3, 4). All four M^H sites are coordinated by five O atoms and one monovalent X^P_M anion, F or OH, with $<M^H-\varphi> = 1.963$ Å. Note the short distances from each M^H cation to each X^O_M anion: $M^H(1)-O(30) = 1.788$ Å, $M^H(2)-O(32) = 1.804$ Å, $M^H(3)-O(31) = 1.792$ Å, and $M^H(4)-O(29) = 1.803$ Å, and the long distances from each M^H cation to each X^P_M anion: $M^H(1)-X^P_M(1) = 2.088$ Å, $M^H(2)-X^P_M(2) = 2.098$ Å, $M^H(3)-X^P_M(3) = 2.103$ Å, and $M^H(4)-X^P_M(4) = 2.098$ Å (Table 3). There are eight tetrahedrally coordinated Si sites occupied solely by Si, with $<Si-O> = 1.621$ Å (Table 4). The cations of the two H sheets give $Ti_4\ Si_8$ p.f.u.

Peripheral sites

In the cámaraite structure, there are six peripheral sites, $4 \times A^P$ and $2 \times B^P$. The $A^P(1)$ and $A^P(2)$ sites are occupied by Ba, and are coordinated by ten O atoms and two monovalent X^P_M anions with $<A^P(1)-O> = 3.023$ Å and by eight O atoms and four monovalent X^P_M anions with $<A^P(2)-O> = 2.932$ Å respectively (Tables 3, 4). The $A^P(3)$ site is occupied by (0.36 Ba + 0.14 K) p.f.u. and is coordinated by eight O atoms and two X^P_M anions, with $<A^P(3)-\varphi> = 2.898$ Å (Tables 3, 4). The $A^P(4)$ site splits into two sites, $A^P(4A)$ and $A^P(4B)$, occupied by Ba and K at 25 and 20%, respectively, and coordinated by nine and eight O atoms with $<A^P(4A)-O> = 2.99$ and $<A^P(4B)-O> = 3.06$ Å (Tables 3, 4). The total content of four A^P sites sums to ~3 a.p.f.u.: $Ba_{2.61}K_{0.34}$, ideally 3 Ba p.f.u.

The two B^P sites are occupied by Na and minor Ca, in accord with the observed site-scattering values (Table 4). The two B^P sites are coordinated by eight O atoms and two monovalent X^P_M anions. For the $B^P(1)$ and $B^P(2)$ sites, the mean distances are 2.629 and 2.626 Å respectively (Table 3). The total content of the two B^P sites is $Na_{0.86}Ca_{0.14}$ (Table 4), ideally 1 Na p.f.u., and the total content of the peripheral sites is Ba_3Na p.f.u.

Anion considerations

There are 28 anion sites, O(1)−O(28), that coordinate the Si sites and they are occupied by O atoms (Table 5). Four anions, O(29)−O(32) [X^O_M in the terminology of Sokolova (2006)], are ligands of three M^O cations and an M^H cation, and they are occupied by O atoms (Table 5). There are four $X^O_A(1-4)$ anions that receive bond-valence contributions from three M^O cations; there are two $X^P_M(1,2)$ anions that receive bond-valence from an M^H cation and three A^P cations, and there is one $X^P_M(3)$ anion that receives bond-valence from two M^H cations, two A^P cations and two B^P cations. Table 5 shows that these seven anions receive bond valences of 1.12−1.29 v.u. (valence unit) and hence are monovalent anions. Chemical analysis gives F = 3.11 a.p.f.u. (table 1, Sokolova *et al*., 2009*a*), and 3.89 OH p.f.u. are required to fill the seven monovalent anion sites. We assign $(OH)_{3.89}F_{3.11}$, ideally $(OH)_4F_3$, to these seven sites. Thus, the composition of a monovalent anion site is ideally $(OH)_{4/7}F_{3/7}$.

We write the anion part of the formula as the sum of: (1) the H sheet − O_{28} (belonging to four Si_2O_7 groups) + (2) the O sheet − four X^O_M and four X^O_A anions, giving O_4 and 4 $[(OH)_{4/7}F_{3/7}]$ + (3) the apical anions of the M^H polyhedra at the periphery of the TS block − three X^P_M cations, giving 3 $[(OH)_{4/7}F_{3/7}]$, ideally $O_{28}O_4(OH)_4F_3$.

We write the structural formula of cámaraite as the sum of the peripheral cations, H-sheet cations, O-sheet cations, (Si_2O_7) groups and anions: $Ba_3Na + Ti_4 + Fe^{2+}_8 + (Si_2O_7)_4 + O_4\ (OH)_4\ F_3$

TABLE 5. Bond-valence (v.u.)* table for cámaraite.

Atom	Si (1)	Si (2)	Si (3)	Si (4)	Si (5)	Si (6)	Si (7)	Si (8)	M^O (1)	M^O (2)	M^O (3)	M^O (4)	M^O (5)	M^O (6)	M^O (7)	M^O (8)	M^H (1)	M^H (2)	M^H (3)	M^H (4)	A^P (1)	A^P (2)	A^P (3)	A^P (4A)	A^P (4B)	B^P (1)	B^P (2)	Σ
O(1)	0.97										0.28	0.30	0.38															1.93
O(2)	1.03																			0.69				0.04	0.01	$0.2^{\times 2}\downarrow$		1.98
O(3)	1.06																		0.60				$0.20^{\times 2}\downarrow$			$0.11^{\times 2}\downarrow$		1.97
O(4)	0.87	0.96																						0.05	0.03			1.97
																								0.04	0.02			
O(5)		0.99										0.27		0.44		0.27												1.97
O(6)		1.05																		0.60			$0.20^{\times 2}\downarrow$				$0.11^{\times 2}\downarrow$	1.96
O(7)		1.02																	0.68					0.04	0.01		$0.2^{\times 2}\downarrow$	1.97
O(8)			1.08															0.60			0.08	0.25						2.01
O(9)			1.01														0.63				0.22							1.97
																					0.11							
O(10)			1.01							0.33		0.33				0.26												1.93
O(11)			0.94	0.96																	0.20							2.10
O(12)				1.00														0.65			0.09	0.22						1.96
O(13)				1.00									0.38		0.32	0.25												1.95
O(14)				1.08													0.62					0.23						2.02
																						0.09						
O(15)					0.97						0.24			0.45	0.30													1.96
O(16)					1.10													0.64				0.24						2.06
																						0.08						
O(17)					1.02												0.65				0.11	0.21						1.99
O(18)					0.95	0.95															0.21							2.11
O(19)						1.08											0.62				0.09	0.25						2.04
O(20)						0.98												0.65			0.22							1.94
																					0.09							
O(21)						0.99			0.38		0.25	0.31																1.93
O(22)							1.06												0.60				$0.20^{\times 2}\downarrow$				$0.11^{\times 2}\downarrow$	1.97
O(23)							0.98		0.39						0.29	0.27												1.93
O(24)							1.01													0.68				0.04	0.01		$0.22^{\times 2}\downarrow$	1.96
O(25)							0.93	0.95																0.04	0.05			2.02
																								0.04	0.01			
O(26)								0.98		0.34	0.29				0.30													1.91
O(27)								1.07												0.60			0.20 $^{\times 2}\downarrow$			0.1 $^{\times 2}\downarrow$		1.97
O(28)								1.01											0.69					0.04	0.01	0.22 $^{\times 2}\downarrow$		1.97
O(29)										0.26			0.16			0.41				1.01								1.84
O(30)												0.35	0.25	0.17			1.05											1.85
O(31)									0.26		0.38			0.16					1.04									1.84
O(32)									0.19	0.26					0.37			1.01										1.83

$X^{O}_{A}(1)$					0.38	0.38		0.37																		1.13
$X^{O}_{A}(2)$									0.36	0.37	0.39															1.12
$X^{O}_{A}(3)$					0.36					0.35		0.41														1.12
$X^{O}_{A}(4)$						0.37	0.39		0.36												0.28	0.27				1.12
$X^{P}_{M}(1)$													0.47									0.11				1.13
$X^{P}_{M}(2)$														0.46							0.27	0.26				1.13
$X^{P}_{M}(3)$															0.45	0.46						0.14	$0.10^{\times 2}\downarrow$	0.02	$0.13^{\times 2}\downarrow 0.13^{\times 2}\downarrow$	1.29
Total	3.93	4.02	4.04	4.04	4.04	4.00	3.98	4.01	1.96	1.94	1.83	1.93	1.89	1.94	1.97	1.87	4.04	4.01	4.06	4.04	1.97	2.35	1.80	0.35	0.15	1.54	1.58	
**Aggr. charge	4.00	4.00	4.00	4.00	4.00	4.00	4.00	4.00	1.94	1.94	1.94	1.94	1.94	1.94	1.94	1.94	4.00	4.00	4.00	4.00	2.00	2.00	1.73	0.50	0.20	1.14	1.14	

* bond-valence parameters are from Brown (1981).
** aggregate charge.
(1) bond-valences from eight M^{O} atoms, $M^{O}(1)$–$M^{O}(8)$, have been calculated on the assumption that each M^{O} atom is represented as follows: 0.64 Fe^{2+} + 0.33 Mn^{2+} + 0.03□, with an aggregate charge of 1.94^{+}.
(2) $M^{H}(1) = M^{H}(2) = M^{H}(3) = M^{H}(4) =$ Ti.
(3) composition of A^{P} and B^{P} sites is in accord with Table 4.

and the ideal formula as $Ba_3NaTi_4Fe_8^{2+}(Si_2O_7)_4O_4(OH)_4F_3$, $Z = 4$. This formula is in accord with the simplified formula given in Sokolova *et al.* (2009*a*).

Topology of the structure

In the structure of cámaraite, the $M^{O}(1-8)$ octahedra form a close-packed octahedral (O) sheet (Fig. 1*a*). In the H sheet, (SiO_4) tetrahedra link *via* common vertices to form (Si_2O_7) groups that are oriented along *b* (Fig. 1*b*,*c*). The (Si_2O_7) groups and M^{H} octahedra share common vertices to form the H sheet. The H_1 sheet consists of $M^{H}(1)$ and $M^{H}(2)$ octahedra and two independent (Si_2O_7) groups, with Si(3), Si(4) and Si(5), Si(6) central atoms respectively (Fig. 1*b*). The H_2 sheet consists of $M^{H}(3)$ and $M^{H}(4)$ octahedra and two independent (Si_2O_7) groups, with Si(1), Si(2) and Si(7), Si(8) central atoms respectively (Fig. 1*c*). The two H sheets are topologically identical except for the peripheral (*P*) sites. In the H_1 sheet, Ba atoms occur at the $A^{P}(1)$ and $A^{P}(2)$ sites (Fig. 1*b*). In the H_2 sheet, Ba and K atoms occur at the $A^{P}(3)$ and $A^{P}(4)$ sites in large voids and Na and Ca atoms occur at the $B^{P}(1)$ and $B^{P}(2)$ sites in small voids (Fig. 1*c*). An O sheet and two adjacent H sheets link through common vertices of (SiO_4) tetrahedra and M^{H} and M^{O} octahedra to form an HOH block parallel to (001) (Fig. 1*d*). In the TS block, (Si_2O_7) groups link to two M^{O} octahedra of the O sheet adjacent along *b*, as in Group II of Sokolova (2006). In cámaraite, there are two intermediate (**I**) blocks. The $\mathbf{I_1}$ block comprises cations at the $A^{P}(1)$ and $A^{P}(2)$ sites which form a close-packed layer (Fig. 1*e*). The $\mathbf{I_2}$ block is composed of cations at the $A^{P}(3,4)$ and $B^{P}(1,2)$ sites which also form a close-packed layer (Fig. 1*f*). In cámaraite, TS blocks connect to each other in two different ways along [001] (Fig. 2*a*):

(1) they link through common vertices of M^{H} octahedra [which are monovalent anions (OH, F)] plus peripheral cations at the A^{P} and B^{P} sites constituting the $\mathbf{I_2}$ block;

(2) they link *via* peripheral cations at the $A^{P}(1)$ and $A^{P}(2)$ sites which constitute the $\mathbf{I_1}$ block and hydrogen bonds between OH groups at the $X^{P}_{M}(1,2)$ sites and O atoms in the H_1 sheets.

Related minerals

There are seven other minerals in Group II: perraultite, jinshajiangite, bafertisite, hejtmanite, yoshimuraite, bussenite and surkhobite, and they

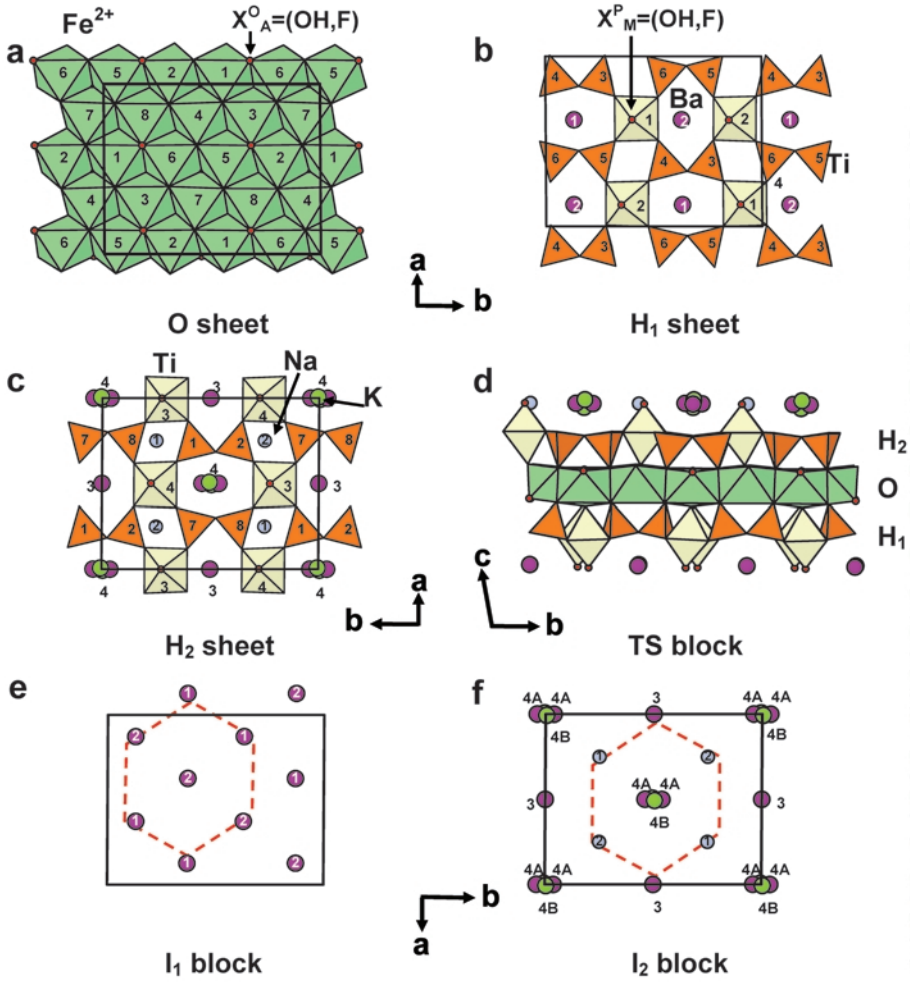

FIG. 1. The crystal structure of cámaraite. The close-packed octahedral (O) sheet (*a*) and the heteropolyhedral H_1 (*b*) and H_2 (*c*) sheets projected onto (001); the TS block projected onto (100) (*d*), a close-packed (**I**) layer of peripheral cations constituting intermediate $\mathbf{I_1}$ (*e*) and $\mathbf{I_2}$ (*f*) blocks projected onto (001). Colour scheme as follows: the SiO_4 tetrahedra are orange; Fe^{2+}-dominant M^O-octahedra and Ti^{4+}-dominant M^H polyhedra are green and yellow; the peripheral Ba-dominant and K-dominant A^P sites are shown as large raspberry and green spheres and they are labelled 1, 2, 3, 4A and 4B respectively; Na-dominant B^P sites are shown as smaller blue spheres labelled 1 and 2; monovalent anions (OH,F) at X^O_A and X^P_M sites are shown as small red spheres. The unit cell is shown by thin black lines. The dashed red lines indicate the six nearest cations around the central one in the **I** layer. In (*a*), labels 1−8 (on green correspond to $M^O(1)$−$M^O(8)$ octahedra respectively. In (*b*) and (*c*), labels 1−4 (on yellow) correspond to $M^H(1)$−$M^H(4)$ octahedra respectively, labels 1−8 (on orange) correspond to Si(1)−Si(8) tetrahedra respectively.

are listed in Table 6. Except for bussenite, these minerals contain an invariant core of the TS block, $M^H_2M^O_4(Si_2O_7)_2X^O_4$, M^H_2 = Ti, Nb; M^O_4 = $(Fe^{2+},Mn)_4$ [for bussenite, $M^O_4 = (Fe^{2+},Mn)_2Na_2$]. There are two types of linkage of TS blocks in these structures. In perraultite, jinshajiangite and surkhobite, TS blocks link *via* common vertices of M^H octahedra (as in astrophyllite-group minerals) and A^P and B^P sites which constitute the **I** block. In bafertisite, hejtmanite, yoshimuraite and bussenite, TS blocks do not link directly, but alternate with **I** blocks. Note that all Group-II

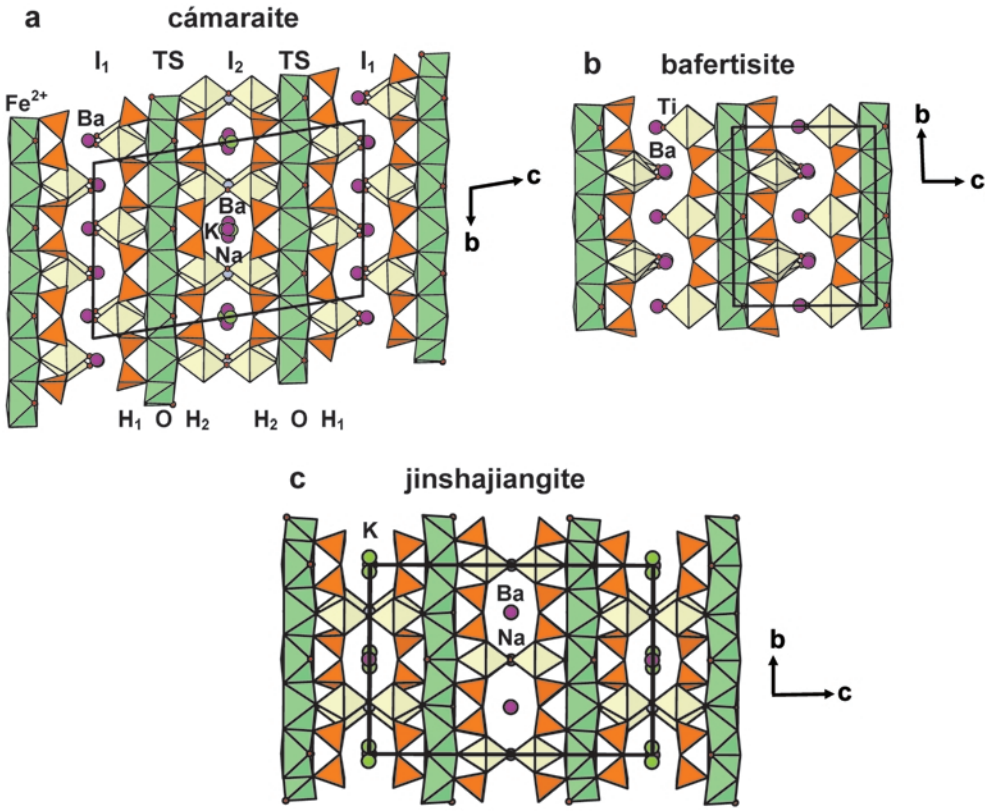

FIG. 2. The crystal structures of: cámaraite (*a*) and related minerals, bafertisite (*b*) and jinshajiangite (*c*) all projected onto (100). Legend as in Fig. 1, Ti-silicate and intermediate blocks are labelled TS and **I** in (*a*), and the sequence of sheets within one TS block is shown in the lower part of the diagram (*a*), i.e. H_1-O-H_2.

minerals listed above have one type of TS block, one type of **I** block, and one type of linkage of TS blocks in the structure.

Cámaraite is the only mineral of Group II with two types of linkage of TS blocks and two types of **I** block in its structure. Compare cámaraite and the two Fe^{2+}-dominant minerals of Group II, bafertisite and jinshajiangite. There are two types of **I** block in cámaraite, $\mathbf{I}_1$ and $\mathbf{I}_2$. The $\mathbf{I}_1$ block is of composition $A^P(1) + A^P(2)_2 = Ba_2$ and is topologically and chemically identical to the **I** block (Ba_2) in bafertisite (Fig. 2*b*). In cámaraite (Fig. 2*a*) and bafertisite (Fig. 2*b*), TS blocks link through Ba atoms of the **I** block plus hydrogen bonding. The $\mathbf{I}_2$ block in cámaraite is of composition $A^P(3,4) + B^P(1,2) = BaNa$ and is topologically and chemically identical to the **I** block (BaNa) in jinshajiangite (Fig. 2*c*). In cámaraite (Fig. 2*a*) and jinshajiangite (Fig. 2*c*), TS blocks link *via* common vertices of M^H octahedra (as in astrophyllite-group minerals) and A^P and B^P atoms which constitute the **I** block.

Sokolova *et al.* (2009*b*) noted that jinshajiangite, $BaNaTi_2Fe^{2+}_4(Si_2O_7)_2O_2(OH)_2F$, and bafertisite, $Ba_2Ti_2Fe^{2+}_4(Si_2O_7)_2O_2(OH)_4$, have (1) a TS block ideally of the same topology and chemical composition, $Ti_2Fe^{2+}_4(Si_2O_7)_2O_2(OH)_2$, and (2) different **I** blocks, BaNa and Ba_2. They emphasized the identical nature of the TS blocks and the similarity of the **I** blocks in jinshajiangite and bafertisite and suggested the possibility of forming atomic and/or nanoscale intergrowths of these two structures resulting in a structure with a TS block of the form $[Ti_2Fe^{2+}_4(Si_2O_7)_2O_2(OH)_2]$ and two **I** blocks of the type found in jinshajiangite and bafertisite.

The crystal structure of cámaraite confirms that prediction. We can write the formula of cámaraite

TABLE 6. Ideal structural formulae and unit-cell parameters for Group II minerals with the TS block.

Mineral	Formula									*a* (Å) α (°)	*b* (Å) β (°)	*c* (Å) γ (°)	Space group	*Z*	Ref.
		$A^P_{1\text{-}2}$	$B^P_{1\text{-}2}$	M^H_2	M^O_4	$(Si_2O_7)_2$		X^O_4							
Perraultite		Ba	Na	**Ti_2**	**Mn_4**	**$(Si_2O_7)_2$**		**$O_2(OH)_2$**	F	10.731 90	13.841 95.06	20.845 90	*C*2	8	(1)
Jinshajiangite		Ba	Na	**Ti_2**	**Fe^{2+}_4**	**$(Si_2O_7)_2$**		**$O_2(OH)_2$**	F	10.6785 90	13.786 94.937	20.700 90	*C*2/*m*	8	(2)
Cámaraite[1]		Ba_3	Na	**Ti_4**	**Fe^{2+}_8**	**$(Si_2O_7)_4$**		**$O_4(OH,F)_4$**	$(OH,F)_3$	10.6965 99.345	13.7861 92.315	21.478 89.993	$C\bar{1}$	4	(3)
Bafertisite		Ba_2		**Ti_2**	**Fe^{2+}_4**	**$(Si_2O_7)_2$**		**$O_2(OH)_2$**	$(OH)_2$	10.6 90	13.64 119.5	12.47 90	*Cm*	4	(4)
Hejtmanite-*P*		Ba_2	Ba_2	**Ti_2**	**Mn_4**	**$(Si_2O_7)_2$**	$(SO_4)_2$	**$O_2(OH)_2$**	$(OH)_2$	5.361 90	6.906 119.8	12.556 90	$P2_1/m$	1	(5)
Hejtmanite-*C*		Ba_2		**Ti_2**	**Mn_4**	**$(Si_2O_7)_2$**		**$O_2(OH)_2$**	$(OH)_2$	5.460 90	7.170 119.9	12.041 90	*Cm*	4	(5)
Yoshimuraite		Ba_2	Ba_2	**Ti_2**	**Mn_4**	**$(Si_2O_7)_2$**	$(PO_4)_2$	**$O_2(OH)_2$**		5.386 89.98	6.999 93.62	14.748 95.50	$P\bar{1}$	2	(6)
Bussenite	$(Na\square)_2$	Ba_2	Ba_2	**Ti_2**	**$(Fe^{2+},Mn)_2Na_2$**	**$(Si_2O_7)_2$**	$(CO_3)_2$	**$O_2(OH)_2$**	$(H_2O)_2F_2$	5.399 102.44	7.016 93.18	16.254 90.10	*P*1	2	(7)
Surkhobite[1,2]		$(Ba,K)_2$	Ca Na	**Ti_4**	**$(Mn,Fe^{2+},Fe^{3+})_8$**	**$(Si_2O_7)_4$**		$O_4(F,OH,O)_6$		10.723 90	13.826 95.00	20.791 90	*C*2	8	(8)

* The invariant core of the TS block, **$M^H_2\ M^O_4\ (Si_2O_7)_2\ X^O_4$**, is shown in bold: M^H = cations of the H sheet; M^O = cations of the O sheet; X^O_4 = anions shared between O and H sheets. For all minerals except for jinshajiangite, cámaraite and surkhobite, ideal structural formulae are from Sokolova (2006).

[1] The formulae for cámaraite and surkhobite are per double minimal cell based on $2t_1$ and $2t_2$ translations $[(Si_2O_7)_4]$;

[2] This formula is taken from Rastvetaeva *et al.* (2008), the ideal structural formula of surkhobite corresponds to that of perraultite.

References[†]: (1) Yamnova *et al.* (1998); (2) Sokolova *et al.* (2009*b*); (3) this work; (4) Guan *et al.* (1963); (5) Rastsvetaeva *et al.* (1991); (6) McDonald *et al.* (2000), Takéuchi *et al.* (1997); (7) Zhou *et al.* (2002); (8) Rastsvetaeva *et al.* (2008), Rozenberg *et al.* (2003).

[†] The latest reference on the structure is the first entry in the numbered list of references.

as the sum of the formulae for jinshajiangite and bafertisite: $BaNaTi_2Fe_4^{2+}(Si_2O_7)_2O_2(OH)_2F$ + $Ba_2Ti_2Fe_4^{2+}(Si_2O_7)_2O_2(OH)_4$ = $Ba_3NaTi_4Fe_8^{2+}(Si_2O_7)_4O_4(OH)_6F$. The latter formula is identical to the ideal formula of cámaraite, $Ba_3NaTi_4Fe_8^{2+}(Si_2O_7)_4O_4(OH)_4F_3$, except for the OH:F ratio.

Figure 3 shows a high-resolution image of a bafertisite-rich zone of cámaraite. The upper right inset shows the selected-area electron-diffraction (SAED) pattern oriented down the $[\bar{1}\bar{1}0]$ direction in a bafertisite area. Stacking disorder at a very local scale can be observed where alternation of TS blocks associated with locally Ba-rich or (Ba-Na)-rich layers builds bafertisite or cámaraite. In other zones, increased Na leads to intergrowths of jinshagiangite and cámaraite (Sokolova *et al.* 2009*a*, fig. 2*a*). Figure 3 also shows that more complex Cam–Baf–Cam–Baf sequences (Cam = cámaraite, Baf = bafertisite) also occur, corresponding to alternation of **I** blocks such as $\mathbf{I}_{Cam}$– $\mathbf{I}_{Baf}$– $\mathbf{I}_{Cam}$– $\mathbf{I}_{Baf}$– $\mathbf{I}_{Baf}$– $\mathbf{I}_{Cam}$– $\mathbf{I}_{Cam}$. This shows that there is no solid solution between the three minerals, as change in composition leads to change in stacking sequences and different topologies. HRTEM data also explain the presence of subsidiary peaks in the electron density map for the cámaraite structure (see discussion above).

Summary

The crystal structure of cámaraite – ideally $Ba_3NaTi_4Fe_8^{2+}(Si_2O_7)_4O_4(OH)_4F_3$ – is triclinic, space group $C\bar{1}$. Cámaraite is the only mineral of Group II which has two types of linkage of TS blocks and two types of **I** block in its structure. There is a close relation between cámaraite and two Fe^{2+}-dominant minerals of Group II, bafertisite, $Ba_2Ti_2Fe_4^{2+}(Si_2O_7)_2O_2(OH)_4$, and jinshajiangite, $BaNaTi_2Fe_4^{2+}(Si_2O_7)_2O_2(OH)_2F$. The three minerals have identical TS blocks. The $\mathbf{I}_1$ and $\mathbf{I}_2$ blocks in cámaraite are of composition Ba_2 and BaNa, respectively, and they are topologically and chemically identical to the **I** blocks in bafertisite and jinshajiangite. In cámaraite, TS blocks link (1) through Ba atoms of the **I** block plus hydrogen bonding as in bafertisite, and (2) *via* common vertices of M^H octahedra (as in astrophyllite-group minerals) and Ba and Na atoms as in jinshajiangite.

Acknowledgements

We thank Joel Grice, Uwe Kolitsch and Mark Welch for careful revision of the manuscript. We thank Mª del Mar Abad Ortega for helping with TEM operation and José Damián Montes Rueda for ion milling. Elena Sokolova thanks Frank C. Hawthorne for critical comments. Fernando Cámara was supported by funding by CNR-IGG through the project TAP01.004.002. He also acknowledges a grant of the Short-term Mobility Program 2008 of the Italian CNR and thanks F.C. Hawthorne for supporting a visiting research period at Winnipeg. Financial support has been provided MEC CGL2007-6674-C02-01/BTE to Fernando Nieto.

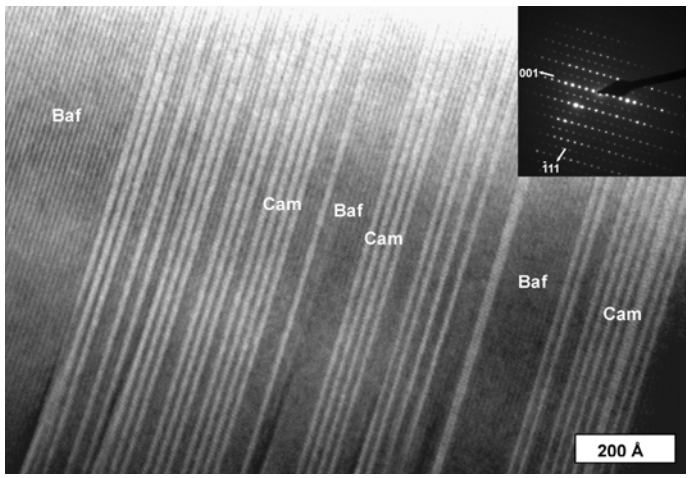

FIG. 3. High-resolution TEM image of cámaraite (Cam) slices in a bafertisite (Baf) matrix. The zone axis is $[\bar{1}\bar{1}0]$. Upper-right inset shows an SAED (selected-area electron-diffraction) image of a bafertisite area.

References

Brown, I.D. (1981) The bond-valence method: an empirical approach to chemical structure and bonding. Pp. 1–30 in: *Structure and Bonding in Crystals II* (M. O'Keeffe and A. Navrotsky, editors). Academic Press, New York.

Cámara, F. and Sokolova, E. (2007) From structure topology to chemical composition. VI. Titanium silicates: the crystal structure and crystal chemistry of bornemanite, a group-III Ti-disilicate mineral. *Mineralogical Magazine*, **71**, 593–610.

Cámara, F., Sokolova, E., Hawthorne, F.C. and Abdu, Y. (2008) From structure topology to chemical composition. IX. Titanium silicates: revision of the crystal chemistry of lomonosovite and murmanite, Group-IV minerals. *Mineralogical Magazine*, **72**, 1207–1228.

Guan, Ya.S., Simonov, V.I. and Belov, N.V. (1963) Crystal structure of bafertisite, $BaFe_2TiO[Si_2O_7](OH)_2$. *Doklady Akademii Nauk SSSR*, **149**, 123–126.

International Tables for X-ray Crystallography Vol. C (1992) Kluwer Academic Publishers, Dordrecht, The Netherlands.

McDonald, A.M., Grice, J.D. and Chao, G.Y. (2000) The crystal structure of yoshimuraite, a layered Ba-Mn-Ti silicophosphate, with comments of five-coordinated Ti^{4+}. *The Canadian Mineralogist*, **38**, 649–656.

Rastsvetaeva, R.K., Tamazyan, R.A., Sokolova, E.V. and Belakovskii, D.I. (1991) Crystal structures of two modifications of natural Ba, Mn-titanosilicate. *Soviet Physics Crystallography*, **36**, 186–189.

Rastsvetaeva, R.K., Eskova, E.M., Dusmatov, V.D., Chukanov, N.V. and Schneider, F. (2008) Surkhobite: revalidation and redefinition with the new formula, $(Ba,K)_2CaNa(Mn,Fe^{2+},Fe^{3+})_8Ti_4(Si_2O_7)_4O_4(F,OH,O)_6$. *European Journal of Mineralogy*, **20**, 289–295.

Rozenberg, K.A., Rastsvetaeva, R.K. and Verin, I.A. (2003) Crystal structure of surkhobite – new mineral from the family of titanosilicate mica. *Crystallography Reports*, **48**, 384–389.

Shannon, R.D. (1976) Revised effective ionic radii and systematic studies of interatomic distances in halides and chalcogenides. *Acta Crystallographica A*, **32**, 751–767.

Sheldrick, G.M. (1997) SHELX-97: *Program for the Solution and Refinement of Crystal Structures*. Siemens Energy and Automation, Madison, Wisconsin, USA.

Sheldrick, G.M. (1998) *SADABS User Guide*, University of Göttingen, Germany.

Sokolova, E. (2006) From structure topology to chemical composition. I. Structural hierarchy and stereochemistry in titanium disilicate minerals. *The Canadian Mineralogist*, **44,** 1273–1330**.**

Sokolova, E. and Cámara, F. (2007) From structure topology to chemical composition. II. Titanium silicates: revision of the crystal structure and chemical formula of delindeite. *The Canadian Mineralogist*, **45**, 1247–1261.

Sokolova, E. and Cámara, F. (2008*a*) From structure topology to chemical composition. III. Titanium silicates: crystal chemistry of barytolamprophyllite. *The Canadian Mineralogist*, **46**, 403–412.

Sokolova, E. and Cámara, F. (2008*b*) From structure topology to chemical composition. VIII. Titanium silicates: the crystal structure and crystal chemistry of mosandrite from type locality of Låven (Skådön), Langesundsfjorden, Larvik, Vestfold, Norway. *Mineralogical Magazine*, **72**, 887–897.

Sokolova, E. and Hawthorne, F.C. (2008*a*) From structure topology to chemical composition. IV. Titanium silicates: the orthorhombic polytype of nabalamprophyllite from Lovozero massif, Kola Peninsula, Russia. *The Canadian Mineralogist*, **46**, 1469–1477.

Sokolova, E. and Hawthorne, F.C. (2008*b*) From structure topology to chemical composition. V. Titanium silicates: the crystal chemistry of nacareniobsite-(Ce). *The Canadian Mineralogist*, **46**, 1493–1502.

Sokolova, E., Abdu, Y., Hawthorne, F.C., Stepanov, A.V., Bekenova, G.K. and Kotel'nikov, P.E. (2009*a*) Cámaraite, $Ba_3NaTi_4(Fe^{2+},Mn)_8(Si_2O_7)_4O_4(OH,F)_7$. I. A new titanium-silicate mineral from the Verkhnee Espe Deposit, Akjailyautas Mountains, Kazakhstan. *Mineralogical Magazine*, **73**, 847–854.

Sokolova, E., Cámara, F., Hawthorne, F.C. and Abdu, Y. (2009*b*) From structure topology to chemical composition. VII. Titanium silicates: the crystal structure and crystal chemistry of jinshajiangite. *European Journal of Mineralogy*, **21**, 871–883.

Takéuchi, Y., Ohashi, Y., Sawada, H. and Haga, N. (1997) Crystal structure of yoshimuraite $(Ba,Sr)_2(S,P)O_4Mn_2OH[Si_2O_7TiO]$, with discussion on its local symmetry. Pp. 253–264 in: *Tropochemical cell-twinning* (Y. Takéuchi, editor). Terra Scientific Publishing Company, Tokyo.

Yamnova, N.A., Egorov-Tismenko, Yu.K. and Pekov, I.V. (1998) Crystal structure of perraultite from the coastal region of the Sea of Azov. *Crystallography Reports*, **43**, 401–410.

Zhou, H, Rastsvetaeva, R.K., Khomyakov, A.P., Ma, Z. and Shi, N. (2002) Crystal structure of new mica-like titanosilicate-bussenite, $Na_2Ba_2Fe^{2+}(TiSi_2O_7)(CO_3)O(OH)(H_2O)F$. *Crystallography Reports*, **47**, 43–46.